SUPPLEMENTAL INFORMATION

Supplemental Figure Legends

Figure S1. Combination screen for synergistic drug combinations in triple-negative BT-20 cells. **(A)** An initial screen of various genotoxins combined with targeted inhibitors was performed in triple-negative BT-20 cells. Dose, time, and combination timing were first screened using the CellTiterGlo assay (Promega). Shown in heatmap form are apoptotic responses for each combination. For each, "PRE" refers to addition of the inhibitor 24 hours before genotoxin; "POST" refers to addition of the inhibitor 4 hours after the genotoxin; "COMBO" refers to the addition of 2 drugs at the same time. All data were collected 8 hours after genotoxin exposure as described in Figure 1. **(B and C)** Apoptotic response of BT-20 cells 8 hours after exposure to genotoxin (as in figure 1) shown in detail for synergistic combinations. **(B)** Apoptotic response and cleaved caspase-8 time course for doxorubicin combined with erlotinib (left) or doxorubicin combined with lapatinib (right). Caspase-8 cleavage was measured by Western blot at indicated times after drug exposure (blot for "E→D" or "L→D" shown). Caspase-8 activity was quantified relative to baseline activation for each treatment at 8 time points, as indicated in the legend. The quantification strategy is described in the supplemtary methods section. **(C)** Apoptotic response for additional synergistic combinations. (left) Camptothecin (CAM) +/- erlotinib (ERL); (middle) CAM +/- lapatinib (LAP); (right) doxorubicin (DOX) +/- gefitinib (GEF). Caspase-8 cleavage 8 hours after genotoxin exposure as monitored by Western blot is shown below for each treament. Detailed analysis of other synergistic combinations are shown in Figure 1 (DOX/ERL) and Figure S7 (DOX/LAP).

Figure S2. Efficacy of erlotinib-doxorubicin Combination requires time-staggered doxing. (A and **B)** Lysates made from BT-20 cells treated with erlotinib for the indicated times were probed for EGFR

activity (p-EGFR Y1173) (A) or activity of signals downstream of EGFR, like ERK (B). Sample blots shown and quantified from 3 independent experiments (data are mean +/- S.D.). **(C)** Increased erlotinib concentration, rather than time-staggered dosing, does not enhance sensitivity to doxorubicin in triple-negative BT-20 cells. Apoptotic response was measured 8 hours after drug exposure by flow cytometry, as described in Figure 1. In all cases, 10μM doxorubicin was co-administered with the indicated amount of erlotinib. These data further support the hypothesis that specific timing/network re-wiring is necessary for enhanced sensitivity to doxorubicin. See also Figure 2. **(D)** Detailed analysis of cell cycle 24 hrs. following drug treatment. Timing of drug combination does not significantly alter cell cycle profile. Cells were treated as in Figure 1, and cell cycle progress monitored using flow cytometry.

Figure S3: Differentially expressed genes following erlotinib treatment in BT-20, MDA-MB-453, and MCF7 cells. Differentially expressed genes (DEGs) following erlotinib treatment for various amounts of time as indicated. Cells were treated with 10μM erlotinib and RNA extracted for microarray analysis. The cut-off for differential gene expression was greater than a 2-fold change and a p-value less than 0.05 (genes that meet both criteria are colored red). P-values were calculated using LIMMA (Smyth, 2004). B score (a measure of significance) is the log of the odds (lods) of differential expression. Data are from 3 biological replicates. **(A-C)** Time course of erlotinib treatment in BT-20 cells. **(D)** 24 hour erlotinib treatment in MDA-MB-453 cells. **(E)** 24 hour erlotinib treatment in MCF7 cells. Expression data can be found in the GEO repository under the accession number GSE30516. See also Figure 3.

Figure S4. A conceptual overview of PLS modeling for the EGFR inhibition/DNA damage dataset. (A) An expanded signaling-response network. This network includes canonical components of

the DNA damage response, together with components in general stress response pathways, and growth factor, cytokine and cell death pathways. Specific targets selected for measurement were based on prior knowledge of the pathway, or by identification of the target protein as a differentially expressed gene in our microarray studies (see also Figure 3 and S3). Briefly, from the identified list of ~2000 DEGs, GSEA and GeneGO were used to identify pathways, molecular signatures, or processes that were significantly altered by long-term erlotinib exposure. Within each pathway, proteins were chosen for study that either 1) function as critical signaling nodes in that particular pathway, or 2) are thought to regulate DNA damage responses or cell death. 1000 antibodies to over 200 targets of interest were tested in both reverse phase protein lysate array format and quantitative Western blot format using a panel of 90 control lysates generated from 30 treatment conditions in 3 different cell lines. Antibodies to targets of interest that were validated to be high fidelity (band at appropriate size; report predicted changes in expression across control lysate panel) were included for computational analysis if treatment-dependent or cell line dependent differences were observed. Proteins whose activity and/or expression were directly measured are boxed in white. BCL2 FAM denotes the BCL2 family members BIM, and BID. **(B)** Simplified explanation of PLS modeling. In this hypothetical example, "signaling space" is comprised of 3 signaling components. Experimental observations (blue) could be plotted with respect to time (as traditionally done and shown in top panel) or plotted in signaling space (as shown below). Dimensionality reduction can be further achieved by identification of principal components, which are defined as latent axes that maximally capture the variance in the dataset. Projection of the original signaling metrics into principal component space is a useful tool for identifying the contribution of each signal to the variance in the dataset. A similar process can be performed on the quantitative measurements of cellular response, and signaling vectors can be regressed against response vectors to identify co-variation between signals and responses. The organization of signaling vectors in signaling

space is determined by methods analogous to those used to cluster gene microarray data. In more complex examples, individual signaling metrics may first be concatenated into a single signaling vectors based on co-linearity. This concatenated signaling space can be further dimensionally reduced as described above. Our data space was comprised of 7560 signaling vectors and 630 response vectors, which were derived from over 47,000 independent measurements. See also Figure 4. **(C-F)** Examples of raw cell response data. **(F)** Autophagy was monitored using automated fluorescence microscopy of cells expressing mCherry-EGFP-LC3B, and quantified using the CellProfiler image analysis software **(G)** Cell viability was quantified using CellTiterGlo. **(H, I)** Cell cycle and apoptosis were quantified by flow cytometry as described in Figures 1 and 2.

Figure S5: PCA and PLS models resolve cell type specific and treatment specific variance in molecular signals. (A) Principal component analysis on signaling measurements from BT-20, MDA-MB-453, and MCF7 cells. Color scheme from Figure 5 is simplified to highlight different cell lines (BT-20 in red, MDA-MB-453 in black, and MCF7 in blue) and treatment-specific responses. Rather than highlighting all six different treatments, those that received doxorubicin in any combination are labeled "+DOX" (open squares) and those treatments that did not receive doxorubicin are labeled "-DOX" (closed circles). "-DOX" treatments include erlotinib, DMSO, and all 0 hour treatment time points. These data highlight that cell line specific information was captured in PC1, while treatment specific information was captured in PC2. NOTE: PC3 did not capture a statistically significant level of variance. **(B-E)** Partial least squares regression analysis of covariance between signaling measurements and cellular fates from BT-20, MDA-MB-453, and MCF7 cells. Simplified color scheme used as described in panels A **(B)** Principal Component 1 (PC1) vs. PC2. **(C)** PC1 vs. PC3 **(D)** PC2 vs. PC3.

(E) Three-dimensional plot highlighting cell-line specific and response specific clusters. These PLS generated data highlight that the co-variance between signals and responses is largely cell type dependent. See also Figure 5. (**F-L**) Measured versus predicted responses for each of the 7 cellular responses monitored in the BT-20 cell line model.

Figure S6: Validation of PLS model generated predictions. (A-C) Additional validation of model generated predictions for targets predicted to have strong, moderate, or negligible influence on apoptosis. Apoptosis was measured 8 hours after the indicated treatment in cells expressing either control RNA (scrambled RNA) or siRNA against indicated target. Data shown are the average of 2 separate siRNAs against the indicated target. (**A**) siRNA targeted against caspase-6 (strong positive covariance with apoptosis in BT-20 and MDA-MB-453 cells; no predicted role in MCF7 cells). (**B**) siRNA targeted against Beclin-1 (moderate negative co-variance with apoptosis in BT-20 cells, but no predicted role in MDA-MB-453 or MCF7 cells). (**C**) siRNA targeted against RIP1 (no predicted role in BT-20 or MDA-MB-453 cells, strong negative co-variance in MCF7 cells). (**D-F**) Validation of knockdown for caspase-6 (D), Beclin-1 (E), and RIP1 (F). Shown for each are control RNA (C), and 2 different siRNAs (1 and 2). Percent knockdown (% k.d.) is calculated relative to control RNA. Actin shown as a loading control (red band in all cases).

Figure S7: Apoptotic response across a panel of breast cancer cell lines reveals a correlation between EGFR activity and sensitivity to erlotinib-doxorubicin combinations in triple-negative cells. (A) Apoptosis was measured by flow cytometry 8 hours after treatment as described in Figure 1. For each protein, basal subtype (A or B) and p53 status are reported (according to (Neve et al., 2006). For p53, protein status is shown in parentheses. EGFR protein levels and EGFR activity (p-EGFR) were

determined by quantitative Western blot with an antibodies directed against EGFR or phospho-EGFR (pY1173). EGFR or p-EGFR values reported are relative to maximum in the cell line panel. For EGFR, shown in parentheses are data reported in Neve et al. when applicable. Chou-Talalay combination index (CI) was used to assess synergy. Mean ± S.D. are shown for 3 independent experiments. (**B**) Dose response profiles for cell lines in which synergistic interactions were found. Data were collected as described in Figure 1G. (**C**) Time-staggered inhibition of HER2 in HER2 driven breast cancer cells in the presence or absence of caspase-8. Apoptosis was measured in HER2 over-expressing BT-474 cells 8 hours after doxorubicin exposure as described in Figure 1. Caspase-8 cleavage was measured by Western blot following the indicated treatments (shown beneath the Control RNA histogram), and caspase-8 knockdown was confirmed using a total caspase-8 antibody (shown beneath the CASP8 siRNA histogram). Percent knockdown (% k.d.) was calculated relative to expression in cells exposed to a control RNA. Lapatinib (LAP; a duel specificity EGFR/HER2 inhibitor.) was used to inhibit HER2. Although synergy was observed for all LAP/DOX combinations in HER2 over-expressing cells, the enhanced sensitivity observed in the time-staggered condition (L→D) relative to the other combinations (D/L or D→L) was mediated by caspase-8 activation as validated by siRNA knockdown. Mean ± S.D. are shown for 3 independent experiments. (**D**) Time-staggered EGFR inhibition in lung cancer cells with high EGFR activity in the presence or absence of caspase-8. Apoptosis was measured in NCI-H358 cells, and data were collected and are presented as in panel C.

Table S1: Complete signaling network and cellular response dataset. Data are in formatted according to the minimal information standard MIDAS, as described in Saez-Rodrigez et al. Columns describe treatments or cell lines (TR), times (DA), or measured targets (DV). Values are the activity/expression measurements normalized as described herein.

EXTENDED EXPERIMENTAL PROCEDURES

Cell culture

All cell lines were obtained from American Type Culture Collection (ATCC) and maintained at low passage (less than 20 passages). Basal media for BT-20 cells was in MEMα + Earle's Salts. A549, MDA-MB-453, MCF7, MDA-MB-231, MDA-MB-468, MDA-MB-436, MDA-MB-157, Hs578T, and Hs578BST were grown in Dulbecco's modified eagles medium (DMEM). Hs578T and Hs578Bst were further supplemented with 10 µg/ml insulin and 30 ng/ml EGF, respectively. HCC-1143, HCC-38, HCC-1500, NCI-1650, NCI-358, BT-474, and BT-549 were grown in RPMI 1640 media, and BT-549 cells were supplemented with 1 µg/ml insulin. Growth media for each line was supplemented with 10% fetal bovine serum (FBS), 2 mm Glutamine, and penicillin/streptomycin. All cells were cultured at 37°C in a humidified incubator supplied with 5% CO_2.

siRNA knockdown

Silencer Select Validated siRNAs were purchased through Invitrogen. For EGFR, si oligos used were: GAUCUUUCCUUCUUAAAGAtt (sense) and UCUUUAAGAAGGAAAGAUCat (antisense); and CCAUAAAUGCUACGAAUAUtt (sense) and AUAUUCGUAGCAUUUAUGGag (antisense). Oligos for caspase-8 were: GAUACUGUCUGAUCAUCAAtt (sense) and UUGAUGAUCAGACAGUAUCcc (antisense); and GAUCAGAAUUGAGGUCUUUtt (sense) and AAAGACCUCAAUUCUGAUCtg (antisense). Oligos for caspase-6 were: GGCUCCUCCUUAGAGUUGAtt (sense) and UGAACUCUAAGGAGGAGCCat (antisense); and GCAUCACAUUUAUGCAUAtt (sense) and UAUGCAUAAAUGUGAUUGCct (antisense). Oligos for Beclin1 were: CAGUUACAGAUGGAGCUAAtt (sense) and UUAGCUCCAUCUGUAACUGtt

(antisense), and GCAGUUGAAAGAAGAGGUUtt (sense) and AACCUCUUCUUUGAACUGCtg (antisense). Oligos for RIP1 were: CCACUAGUCUGACGGAUAAtt (sense) and UUAUCCGUCAGACUAGUGGta (antisense), and GCAAAGACCUUACGAGAAUUtt (sense) and AUUCUCGUAAGGUCUUUGCtg (antisense). For transfection in human cell lines, Lipofectamine RNAiMAX was used according to manufacturer's instructions. Dose titration and time course experiments were performed to determine that optimal knockdown efficiency, which in all experiments was 5nM siRNA for 48 hours.

Cellular response assays

Apoptosis. $1x10^6$ cells were seeded in a 10 cm dish 24 hours prior to the experiment. For treatments involving doxorubicin and/or erlotinib, both drugs were used at a final concentration of 10 μM, unless otherwise noted. Following the treatment time course, cells were washed in PBS, trypsinized, and fixed in 4% paraformaldehyde (PFA) in PBS for 15 minutes at room temperature (RT), then resuspended in ice cold methanol and incubated overnight at -20°C. Cells were then washed twice in PBS + 0.1% Tween and stained with antibodies directed against cleaved forms of caspase-3 and PARP (BD Pharmingen). Secondary antibodies conjugated to Alexa dyes (488 and 647) were used for visualization in a BD FacsCaliber flow cytometer (Molecular Probes). Data reported are always percent cleaved-caspase-3/cleaved-PARP double positive cells.

Cell cycle analysis. Cells were plated and treated as above, but fixed in 70% ethanol in PBS overnight at -20°C, permeabilized with PBS containing 0.25% Triton X-100 for 20 minutes at 4°C, blocked with 1% bovine serum albumin in PBS, and incubated with anti-phospho-Histone H3 antibody for 1 hour (Millipore). Following washing, cells were incubated with Alexa488-conjugated secondary antibody for 1 hour on ice, washed, and resuspended in PBS containing 50 μg/ml propidium iodide (PI)

prior to analysis on a BD FACScaliber flow cytometer. Data were analyzed using the FloJo software, and the Dean-Jett-Fox algorithm for cell cycle analysis.

Cell viability/proliferation. Cells were plated at 5,000 cells/well in 96-well optical bottom plates. Metabolic viability was determined using CellTiterGlo (Promega) according to the manufacturer's protocol. Linearity of the luminescent signal was validated for each cell line used, and data were validated by comparison to total cell count as determined by a Coulter counter.

Autophagy. Cells were stably transfected with pBABE-mCherry-EGFP-LC3B (Addgene Plasmid 22418), which reports activation of autophagy and maturation of autophagic particles to autolysosomes. Expression of this plasmid was determined to have no effect on cell growth rate, apoptosis, or chemosensitivity (data not shown). Cells were seeded onto 18 mm^2 coverslips and treated with erlotinib or doxorubicin or both for the indicated times. Cells were then fixed in 3% PFA and 2% sucrose for 15 minutes at RT, and stained for 10 minutes with whole cell blue stain according to manufacturer's protocol (Thermo Scientific). Images were collected on an Applied Precision DeltaVision Spectris automated microscope and deconvolved using Applied Precision SoftWoRx software. Deconvolved image projections were analyzed using CellProfiler, to identify total cells as well as autophagic cells. A modified "speckle counter" pipeline was used as described previously (Carpenter et al., 2006). Briefly, whole cell blue signal was used to segment each image into individual cells. Number of GFP or mCherry LC3 puncta were counted per cell, and cells were counted as "autophagic" if the number of GFP and mCHERRY puncta significantly increased relative to untreated cells (Mizushima et al., 2010). Approximately 100 cells were counted in a double blind fashion per condition, and percent autophagic cells reported from 3 independent experiments.

Western blotting and antibodies

Cell lysates were prepared in a manner that would allow samples to be used for both Western blot analysis and reverse phase protein microarray. Cells were washed twice in PBS and lysed directly on the plate in a buffer containing 50 mM Tris-HCl, 2 % SDS, 5% glycerol, 5 mM EDTA, 1 mM NaF, 10 mM β-glycero-phosphate, 1 mM PMSF, 1 mM Na_3VO_4, containing phosphatase and protease inhibitors (Roche complete protease inhibitor tablets and PhosSTOP tablets). Crude lysates were filtered using an AcroPrep 96 well 3.0 μm glass fiber/0.2 μm BioInert filter plate (Pall), and normalized for protein content using the BCA protein assay (Pierce). For Western blots, lysates were run on 48-well pre-cast gels and transferred using a semi-dry fast transfer apparatus onto nitrocellulose membranes (i-PAGE, E-BLOT, Invitrogen). Blots were blocked in Odyssey Blocking Buffer (LiCOR Biosciences), incubated overnight with primary antibody, stained with secondary antibodies conjugated to an infrared dye, and visualized using an Odyssey flat bed scanner (LiCOR Biosciences).

Most antibodies used in this study were purchased from Cell Signaling Technologies, including those targeting γH2AX, SMAC, p-4EBP1, Beclin, p53, p-Erk, p-C-abl, cleaved caspase-6, cleaved-caspase-9, Cdc25C, p-Chk1(pSer-317), p-Chk1(pSer-345), p27, p-AKT (pS-473), p-JNK, p-p38, BIM, BID, RIP1, Cyclin D1, p-STAT3, p-p53 (Ser-15), cleaved caspase-8, EGFR, HER2, IKBα, PUMA, p-Wee1, p-HSP27, p-S6, and p-S6K. Antibodies against β-actin were purchased from Sigma, antibodies against DUSP6 and p-DAPK1 (308) from Abcam, antibodies against DAPK2 from Abgent), and antibodies against p-Histone H3 (Ser-10) were from Millipore. Antibodies against p-EGFR (pY1173) were purchased from Epitomics.

Data generated by quantitative Western blot was pre-processed prior to use in computational modeling. Raw signals for each protein target of interest were quantified and background subtracted using the Li-COR Odyssey software, divided by β-actin signals to normalize for loading differences,

then each normalized signal was divided by a reference sample contained on each gel, for gel-to-gel normalization. Reference samples (i.e. positive controls) were chosen for each antibody from a panel of 90 control lysates. For use in Datarail, signal averages were calculated from biological triplicate experiments, the maximum/minimum signals identified, and the data were then plotted according to fold change across all cell lines and all treatment conditions (see Figure 4). Antibodies that did not report significant levels of variance were omitted.

Reverse phase protein microarray

Reverse phase protein microarrays were printed on a fee-for-service basis through Aushon Biosystems. Validation of antibodies, staining and analysis of array data were performed as described previously in (Sevecka and MacBeath, 2006).

Immunofluorescence Microscopy

Cells were seeded onto 18mm^2 coverslips and either mock treated or treated with doxorubicin and/or erlotinib for the indicated times. Cells were then fixed in 3% PFA and 2% sucrose for 15 min at RT and permeabilized with 20mM Tris-HCl (pH7.8), 75mM NaCl, 300mM sucrose, 3mM $MgCl_2$, and 0.5% Triton-X-100 for 15min at RT. Slides were stained with primary antibody targeting either p-H2AX or 53BP1 at 4°C overnight. Following washing, secondary antibodies were applied for 3 hrs at RT. After washing, cells were stained with DAPI for 20 minutes, washed and mounted using Prolong Gold and allowed to dry over-night. Images were collected on an Applied Precision DeltaVision Spectris automated microscope and deconvolved using Applied Precision SoftWoRx software. Deconvolved image projections were analyzed using CellProfiler, to identify nuclei and foci. A modified version of the cell profiler pipeline "speckle counter" was used for this analysis as described herein for

quantification of autophagic flux. Data reported are integrated intensity of pH2AX or 53BP1 foci per nucleus.

Doxorubicin Influx Measurements

Doxorubicin is a naturally fluorescent molecule. Measurement of doxorubicin retention was performed as described previously by(Turner et al., 2006). Doxorubicin and erlotinib were both added to a final concentration of 10 μM.

RNA expression analysis by microarray analysis

RNA was extracted from cells using the RNAeasy Kit (Qiagen). Affymetrix Human U133 Plus 2.0 microarrays were hybridized, labeled and processed on a fee-for-service basis through the BioMicro Center at MIT. Microarray data were obtained from 3 independent biological replicates per time point. Detailed analysis of microarray data was performed with help from the Bioinformatics Core Facility at the Koch Institute at MIT. Expression data can be found in the GEO repository under the accession number GSE30516.

Soft agar growth assay

Soft agar growth assays were performed as described previously by Sapi et al. (1998).

Chemicals

Doxorubicin hydrochloride (doxorubicin), PD98059, BMS-345541, rapamycin, wortmannin, taxol, cisplatin, etoposide, camptothecin, and temezolomide were purchased through Sigma; Erlotinib,

Gefitinib, and lapatinib were purchased through LC Laboratories; NVP-BEZ235 was a generous gift from Dr. Lewis Cantley (Harvard Medical School).

Computational modeling and statistics

Unless otherwise noted, all statistical analyses were performed using Graphpad Prism version 4.0, and graphs were created using Microsoft Excel, Spotfire, Matlab, DataRail (Saez-Rodriguez et al., 2008), or SIMCA-P. Analysis of flow cytometry data was performed using FloJo. Analysis of RNA expression microarray data was performed either using GSEA or using GeneGO as indicated. For GSEA analysis, mRNA expression data was analyzed using GSEA databases C2, C4, and C5 (see www.broadinstitute.org/gsea/msigdb for details). Importantly, pathways in GeneGO are not based on GO terms, but rather built from the primary literature sources.

Data Driven Modeling. Data driven modeling and the application of partial-least squares to biological data have been described in detail previously (Janes and Yaffe, 2006). In PLS modeling, the goal is to predict Y (responses) from X (signals) and to describe their common structure. The data were divided into two matrices: E (a matrix containing the X variables) and F (a matrix containing the Y variables). In our study the dimensions of E are 648 x 35 (6 treatments x 3 cell lines x biological triplicate measurements x 12 time points; 35 signals) and the dimensions of F are 648 x 7 (7 cellular responses). In this study, all data were mean centered and unit variance scaled to non-dimensionalize the different measurements. PLS regression analyses was performed using the program SIMCA-P (Umetrics). The PLS model was constructed using the following iterative formulas:

$E_1 = X - t_1 p_1^T$; $E_2 = E_1 - t_2 p_2^T$, $t_2 = E_1 w_1$; $E_i = E_{i-1} - t_i p_i^T$, $t_i = E_{i-1} w_i$

$F_1 = Y - b_1 t_1 q_1^T$; $F_2 = F_1 - b_2 t_2 q_2^T$; $F_i = F_{i-1} - b_i t_i q_i^T$

E represents the residual of the principal component, with score vector t, weight vector w, loading vector p, and ^{T} represents transpose. F represents the residuals of the dependent principal component, with score vector t, loading vector q, and b represents the inner relation between the independent and dependent principal components. Model predictions were made via cross-validation by leaving out a random sample of $1/6^{th}$ of the observations and predicting that $1/6^{th}$ from the remaining $5/6^{th}$ of the data. The process was reiterated until each of the data were omitted and predicted. Model fitness was calculated using R^2, Q^2, and RMSE, which were calculated as described previously by Gaudet et al. (2005). Variable importance in projection (VIP) was calculated as described by Janes et al. (2008).

Xenograft Tumor Model

For *in vivo* tumor regression assays, 10^7 BT-20 cells in 0.1 ml of PBS were mixed 1:1 with matrigel on ice, injected subcutaneously into the hindflanks of nude mice (NCR nu/nu, Taconic), and tumors were allowed to form for 7 days. Mice were then treated with doxorubicin (4 mg/kg, intraperitoneal administration), or a combination of doxorubicin and erlotinib (25 mg/kg, intraperitoneal adminstration). For those mice given a combination of the 2 drugs, erlotinib was either given at the same time as doxorubicin (D/E condition), or given 8 hours prior to doxorubicin (E→D condition). Tumors were monitored for 14 days after the treatment phase, and volume estimated using the ½ L x W^2 formula. Experiments were performed with 4 mice per experimental condition, and data were plotted as mean ± SEM. These experiments were approved by the Massachusetts Institute of Technology Committee on Animal Care (CAC).

REFERENCES

Carpenter, A.E., Jones, T.R., Lamprecht, M.R., Clarke, C., Kang, I.H., Friman, O., Guertin, D.A., Chang, J.H., Lindquist, R.A., Moffat, J., *et al.* (2006). CellProfiler: image analysis software for identifying and quantifying cell phenotypes. Genome Biol *7*, R100.

Janes, K.A., and Yaffe, M.B. (2006). Data-driven modelling of signal-transduction networks. Nat Rev Mol Cell Biol *7*, 820-828.

Mizushima, N., Yoshimori, T., and Levine, B. (2010). Methods in mammalian autophagy research. Cell *140*, 313-326.

Neve, R.M., Chin, K., Fridlyand, J., Yeh, J., Baehner, F.L., Fevr, T., Clark, L., Bayani, N., Coppe, J.P., Tong, F., *et al.* (2006). A collection of breast cancer cell lines for the study of functionally distinct cancer subtypes. Cancer Cell *10*, 515-527.

Saez-Rodriguez, J., Goldsipe, A., Muhlich, J., Alexopoulos, L.G., Millard, B., Lauffenburger, D.A., and Sorger, P.K. (2008). Flexible informatics for linking experimental data to mathematical models via DataRail. Bioinformatics *24*, 840-847.

Sevecka, M., and MacBeath, G. (2006). State-based discovery: a multidimensional screen for small-molecule modulators of EGF signaling. Nat Methods *3*, 825-831.

Smyth, G.K. (2004). Linear models and empirical bayes methods for assessing differential expression in microarray experiments. Stat Appl Genet Mol Biol *3*, Article3.

Turner, J.G., Gump, J.L., Zhang, C., Cook, J.M., Marchion, D., Hazlehurst, L., Munster, P., Schell, M.J., Dalton, W.S., and Sullivan, D.M. (2006). ABCG2 expression, function, and promoter methylation in human multiple myeloma. Blood *108*, 3881-3889.

Supplemental Figure 1

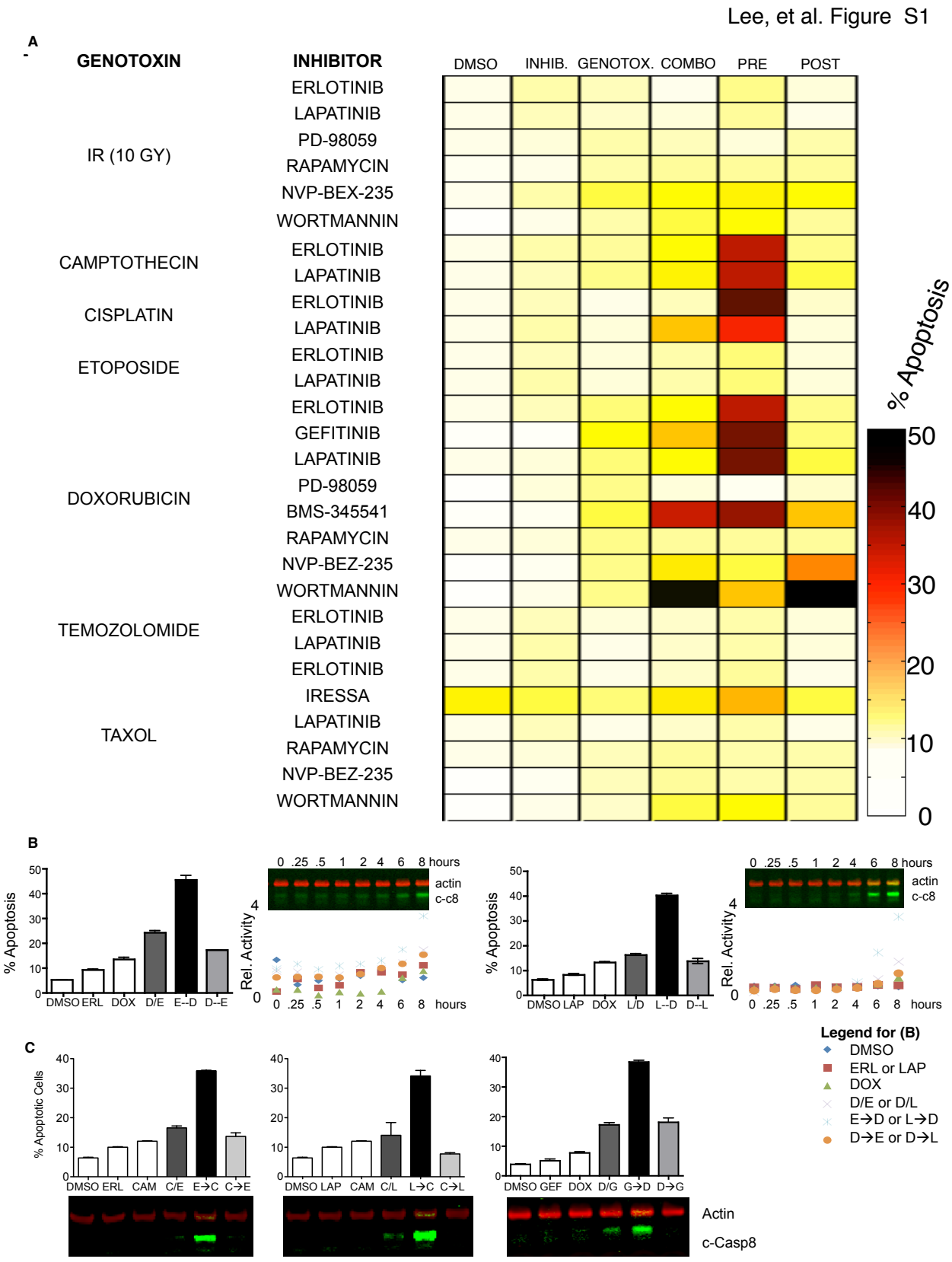

Figure S1: Combination Screen for Synergistic Drug Combinations in Triple-Negative BT-20 Cells, Related to Figure 1

Supplemental Figure 2

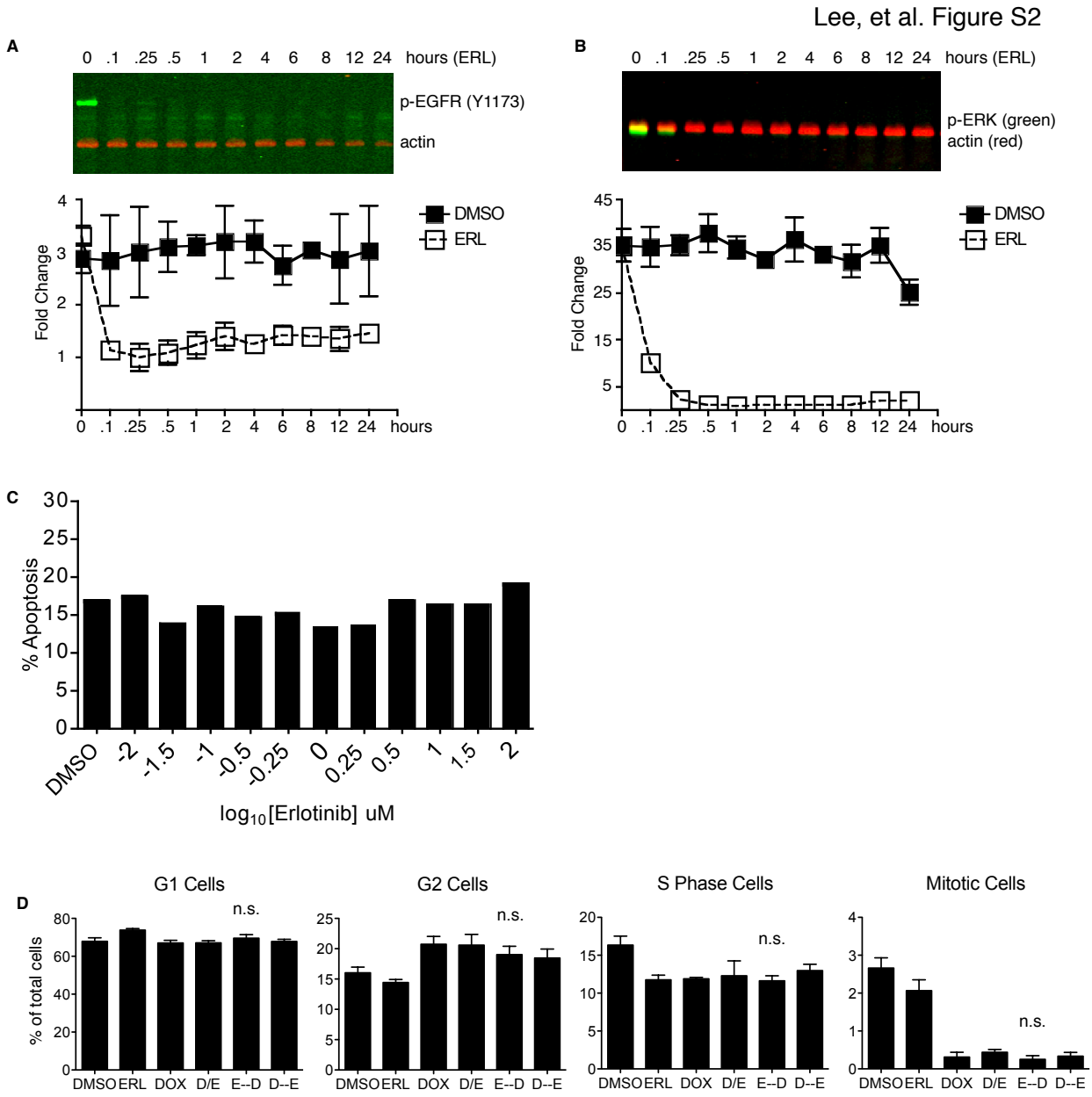

Figure S2: Efficacy of Erlotinib-Doxorubicin Combination Requires Time-Staggered Dosing, Related to Figure 2

Supplemental Figure 3

Lee, et al. Figure S3

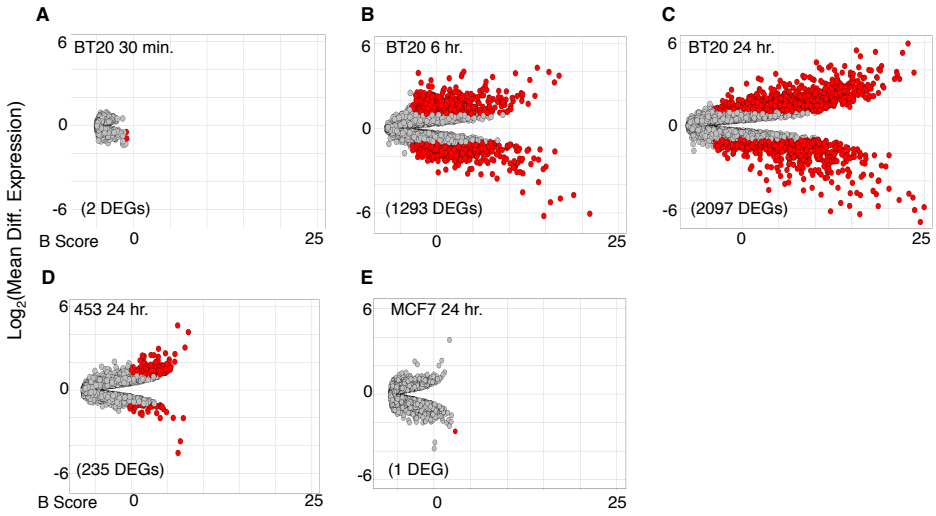

Figure S3: Differentially Expressed Genes Following Erlotinib Treatment in BT-20, MDA-MB-453, and MCF7 Cells, Related to Figure 3.

Supplemental Figure 4

Lee, et al. Figure S4

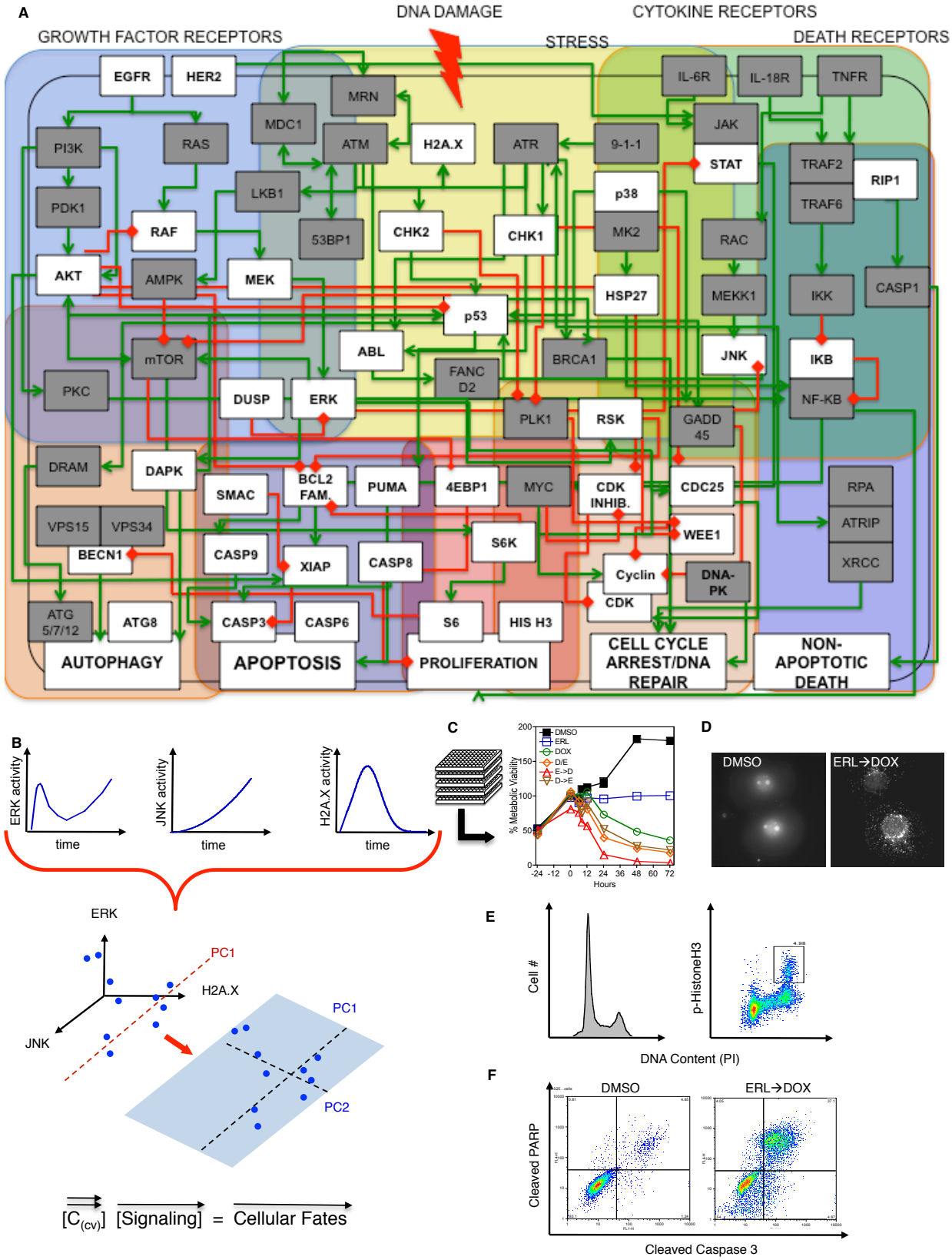

Figure S4: A Conceptual Overview of PLS Modeling for the EGFR Inhibition/DNA Damage Dataset, Related to Figure 4.

Supplemental Figure 5

Lee, et al. Figure S5

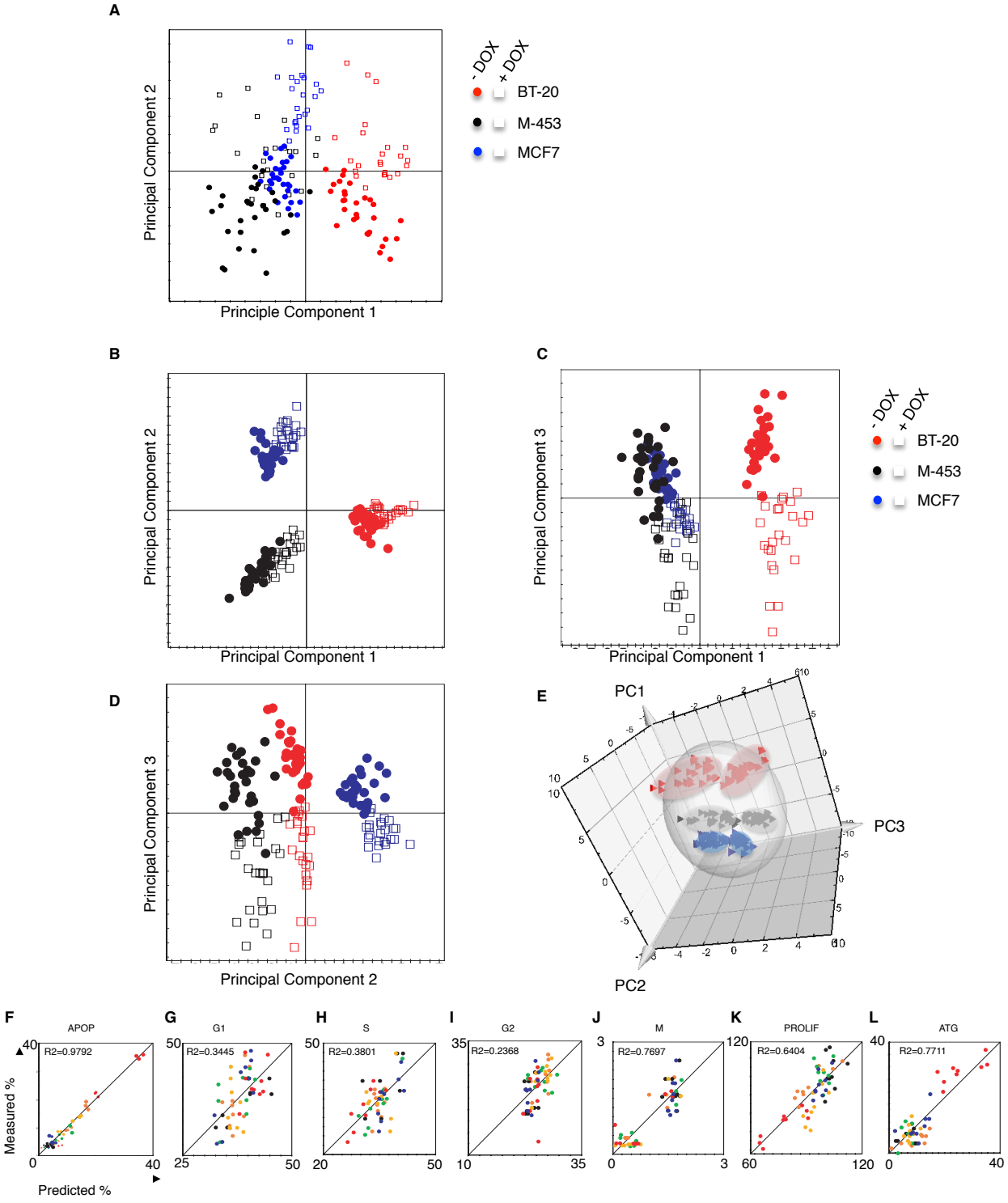

Figure S5: PCA and PLS Resolves Cell Type Specific and Treatment Specific Variance in Molecular Signals, Related to Figure 5.

Supplemental Figure 6

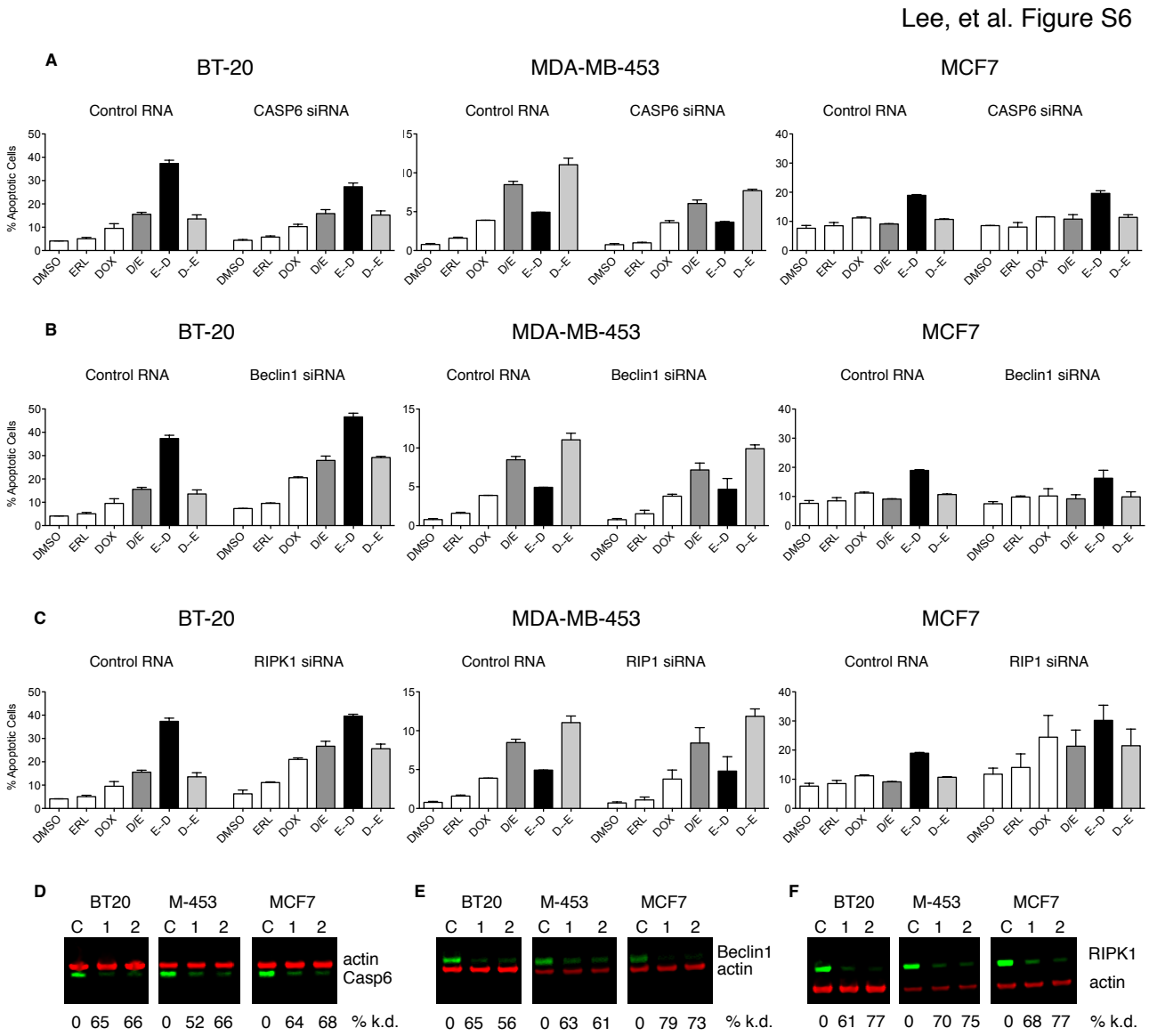

Figure S6: Validation of PLS model generated prediction, Related to Figure 6

Supplemental Figure 7

Lee, et al. Figure S7

A

	MDA-MB-468	BT-20	HCC-1143	Hs-578T	MDA-MB-231
SUBTYPE	TNBC (Basal A)	TNBC (Basal A)	TNBC (Basal A)	TNBC (Basal B)	TNBC (Basal B)
p53 (protein)	+/+ (R273H)	+/+ (WT)	+/+ (WT)	+/m (V157F)	+/GOF (R280K)
EGFR	100 (n/a)	25.09 (3011)	59.79 (7175)	28.78 (3454)	49.95 (5994)
p-EGFR	100	67.85	28.18	17.68	17.13
SYNERGY (CI)	YES (0.16)	YES (0.21)	YES (0.36)	YES (0.15)	NO (0.80)

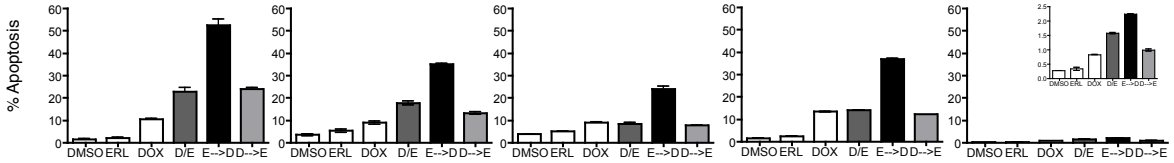

	HCC-38	BT-549	MDA-MB-436	MDA-MB-157	HCC-1500
SUBTYPE	TNBC (Basal B)	TNBC (Basal B)	TNBC (Basal B)	TNBC (Basal B)	TNBC (Basal B)
p53 (protein)	+/m (R273L)	+/m (R249S)	-/-	-/m	+/- (WT)
EGFR	18.68 (2241)	36.21 (4345)	25.50 (n/a)	75.28 (9034)	35.56 (8737)
p-EGFR	15.47	12.71	8.84	2.76	0.00
SYNERGY (CI)	NO (0.72)	NO (0.68)	NO (0.97)	NO (0.98)	NO (0.83)

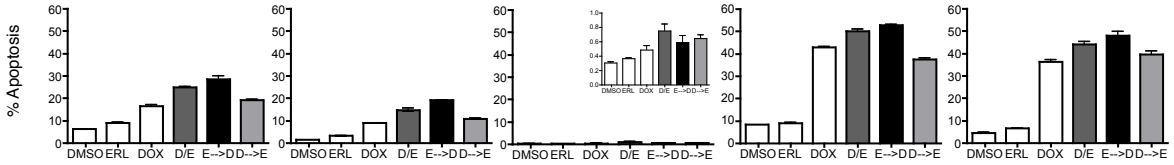

B

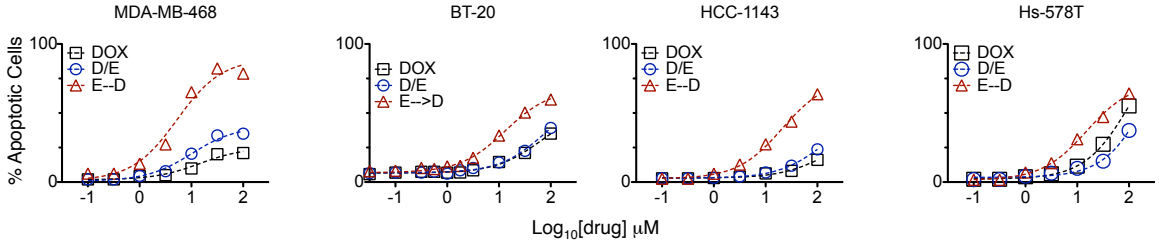

C

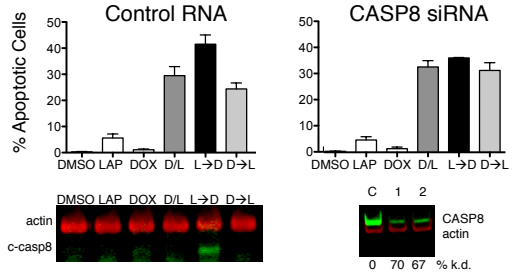

D

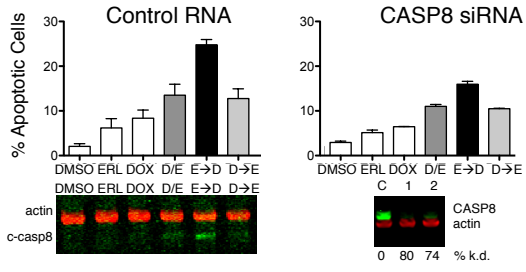

Figure S7: Apoptotic Response Across a Panel of Breast Cancer Cell Lines Reveals Correlation Between p-EGFR and Sensitivity to Erlotinib-Doxorubicin Combinations in Triple-Negative Cells, Related to Figure 7